https://doi.org/10.55343/CogSust.20674

Optimal photo overlap for road accident documentation and reconstruction applying UAV imagery

Gábor Vida
https://orcid.org/0000-0002-2682-808X
Department of Automotive Technologies, Faculty of Transportation Engineering and Vehicle Engineering,
Budapest University of Technology and Economics
Budapest, Hungary
vida.gabor@kjk.bme.hu

Nóra Wenszky
https://orcid.org/0000-0002-6490-2391
Centre of Modern Languages, Faculty of Economic and Social Sciences,
Budapest University of Technology and Economics
Budapest, Hungary
wenszky.nora@gtk.bme.hu

Gábor Melegh
Department of Automotive Technologies, Faculty of Transportation Engineering and Vehicle Engineering,
Budapest University of Technology and Economics
Budapest, Hungary
melegh.gabor@kjk.bme.hu

Árpád Török*
https://orcid.org/0000-0002-8573-6345
Department of Automotive Technologies, Faculty of Transportation Engineering and Vehicle Engineering,
Budapest University of Technology and Economics
Budapest, Hungary
torok.arpad@kjk.bme.hu

Abstract

This study investigates the optimal photo overlap for documenting and reconstructing road accident sites using drone imagery. While a general recommendation for drone imagery overlap stands at 60–80%, this research aims to determine the minimum acceptable overlap required to generate a precise 3D point cloud suitable for forensic road accident simulation. A DJI Mavic Air 2 drone captured images at 2-meter intervals over a junction and a connecting road segment from varying altitudes, following the same flight path. The experiment systematically excluded images from the original dataset, processing photo sets taken at 2, 4, 6, 8, and 10-meter intervals. The corresponding point clouds were evaluated for accuracy and fragmentation. Comparisons were made regarding the number of images, the size of image sets and processing times. Additionally, 3D mesh surfaces were generated in the Virtual Crash software, and their quality was assessed. Results revealed that a 50% overlap was adequate for generating satisfactory

https://doi.org/10.55343/CogSust.20674

3D simulation environments, thereby reducing size of the raw data, the point cloud and processing time considerably. This finding is significant for forensic experts seeking efficient methods of road accident scene reconstruction, emphasizing the practicality of lower photo overlap in such scenarios.

Keywords

image overlap, mesh surface, drone, accident documentation, terrain

1. Introduction

In contemporary contexts, unmanned aerial vehicles (UAVs), i.e. drones are applied for diverse tasks across varied environments. The use of drones in surveying and monitoring reduces the need for large teams and heavy machinery, lowering fuel consumption and greenhouse gas emissions, thus contributing to sustainability. Drones enable precise data collection for a number of purposes, ranging from maritime applications (Nomikos et al., 2023), through topographic modelling (Török et al., 2020) and road traffic monitoring (Bisio et al., 2022), to agricultural land monitoring (El Hoummaidi, 2021) and checking on photovoltaic plants (Michail, 2024). In order to ensure that the processed images yield a satisfactory 3D point cloud and a 2D orthomosaic, the acquired images should overlap both along the drone's trajectory (forward overlap) and laterally (side overlap). This overlap facilitates the image processing software in creating a cohesive image through the identification of tie points, i.e., features automatically recognized on two or more adjacent images.

Singh and Fazier (2018) in their meta-analysis of 108 publications on unmanned aircraft system (UAS) imagery warn that there are no standardized practices for image collection and processing. Based on their extensive literature review, they concluded that the observed studies adopted a broad spectrum of overlap values. Specifically, the forward overlap ranged from 60% to 95%, while side overlap spanned from 40% to 90%. Out of the 108 studies analyzed by them, they found none that explicitly stated how terrain characteristics and optimal image overlap are related. Nonetheless, they hypothesize that for flat terrains (i.e. areas with little variation in altitude) higher overlaps are required to ensure that enough tie points are found for 3D point cloud generation.

As Wang et al. (2022) remark, the number of studies with the objective of determining the optimal overlap for missions with UAVs is considerably low. Nevertheless, when confronted with constraints such as limited image processing time or the storage capacity of the computing systems responsible for handling UAV-captured images, an optimal trade-off point must be identified between the quality of the point cloud and the number of images captured in a mission (and hence, the degree of overlap). This means, the minimum overlap of images that yield a satisfactory 3D point cloud and orthomosaic should be determined (cf. Dandoiset al., 2015). The definition of what qualifies as satisfactory highly depends on the type of terrain (Singh & Frazier, 2018), and the objectives of the UAV mission.

One of the applications of UAVs for data collection is road accident scene documentation (Desai et al., 2022), which is in the focus of this research. UAV images at accident sites are typically captured with high overlaps (80–90%) (Pádua et al, 2020; Mat Amin et al., 2020; Zulkifli and Tahar, 2023; Pérez et al., 2024). A road accident site is generally diverse, including vehicles, debris, objects along the road and surrounding buildings or vegetation. Meanwhile, variations in elevation are generally low. Consequently, it is hypothesized that lower forward overlaps between UAV-captured images may produce a satisfactory point cloud (cf. Section 3.1 for a more detailed analysis).

https://doi.org/10.55343/CogSust.20674

This study explores the minimum forward overlap of UAV captured images required to generate point clouds that are still sufficient for the purpose of accident site documentation and reconstruction. In a field test, images were captured with a DJI Mavic Air2 commercial-grade non-RTK UAV in three flights at three altitudes over a public road junction, without the application of ground control points (GCP) (Stott et al., 2020). The images were processed with Agisoft Metashape software in multiple rounds, systematically reducing the the number of images in each round. The resulting point clouds were evaluated for horizontal accuracy and gaps. Additionally, a triangular mesh surface was created for each point cloud using Virtual Crash accident simulation software. The quality of this mesh, which may be applied as a simulation environment, was also checked.

2. Materials and methods

For the test flights, a commercial-grade non-RTK UAV was applied. The DJI Mavic Air 2 drone's major specifications are given in Table 1. The model was chosen due to the simplicity of operation and low cost.

Table 1. Specifications of the DJI Mavic Air 2 drone (DJI, n.d.).

Camera Model	CMOS Sensor [inch]	Resolution	Pixel size [µm]	Focal length [mm]
DJI FC3170	1/2	4000 × 2250	1.77 × 1.77	4.5

The experiments were conducted at the intersection of the lower ranking Road 5207, running on an embankment, and an unpaved roadway in Hungary (47.23518881,19.11902875). The road segments that were recorded are fully paved on both roads (Figure 1). The specific site was selected due to the relatively low traffic, the absence of arboreal obstructions, and the presence of clearly demarcated road delineations. It is also imperative to note that Road 5207 is delineated by lower terrain on both sides.

Figure 1. The site of the experiment

https://doi.org/10.55343/CogSust.20674

In order to be able to check horizontal accuracy of the point clouds, chartreuse markers were placed next to the road, at 2.00 m from each other (Figure 2). The distance between the markers was measured with a laser measure.

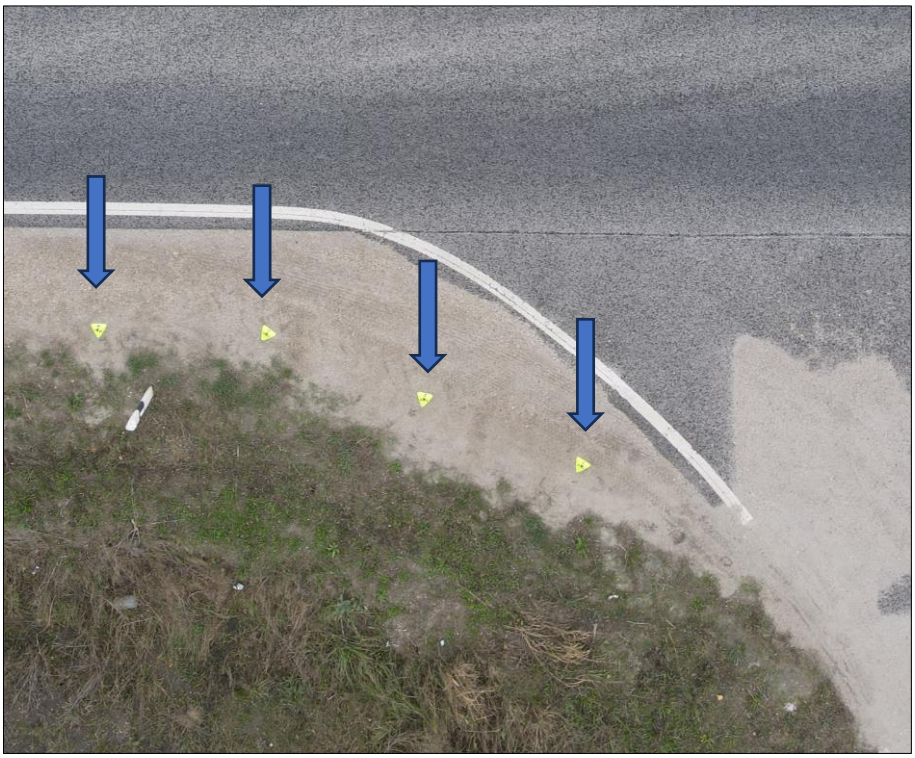

Figure 2. Chartreuse markers along the road section

Three flights were administered, at distinct altitudes: 7.5, 10, and 13 meters, respectively. Apart from the variations in altitude, the routes in the three flights were identical (Figure 3). These missions were pre-programmed with the Litchi software (Litchi, 2023) to ensure that the photographs were taken at identical geographical locations across all altitudes.

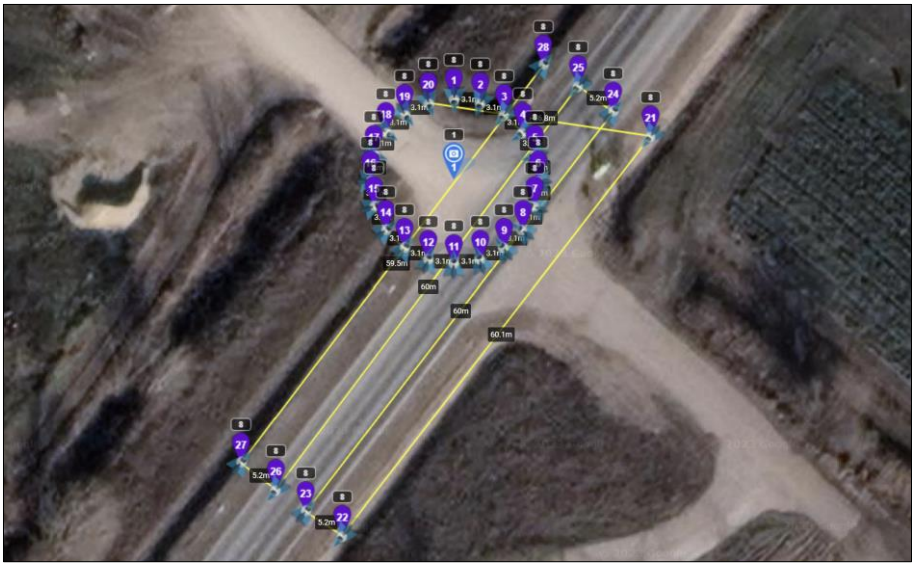

Figure 3. The route of the UAV in the test runs. Yellow lines show the route, and purple circles depict the points where the UAV changed direction. In the circular route, photos were taken at the places marked by purple circles

https://doi.org/10.55343/CogSust.20674

In the initial phase of each mission (Block 1), the UAV followed a circular trajectory centered around an imaginary point of interest (POI) situated at 1 m above ground level at the intersection. The camera was oriented towards this POI, at altitudes of 7.5, 10, and 13 meters, with oblique camera angles (-36°, -49° and -57°, respectively). When the circular path was completed, the UAV proceeded to the second part of the mission. In the second phase (Block 2), the UAV traversed a linear stretch of 60 meters along the paved road, encompassing the junction itself, through four parallel flight lines. While following this grid route, the camera was directed toward the ground with a vertical axis. As a result, oblique images were captured along the circular path over the junction, while nadir images were taken while the drone flew over the extended road segment, following a single grid pattern. The UAV captured images at every 2 meters in all missions (Table 3).

The grid path (Block 2) was combined with a circular path (Block 1) in order to avoid systematic point cloud deformations, such as doming and bowling (Nesbit and Hugenholtz, 2019; Sanz-Ablanedo et al., 2020; James et al., 2020). However, for the purposes of the present study, namely overlap investigations, only images captured during Block 2 were utilized.

Table 2. Main data of the missions

Diameter of circular path [m]	Length of gird paths [m]	Total length of a mission [m]	Image no. Blocks 1+2	Image no. Block 2	Flying time [min:sec]
20	60	341	153	132	8:00

The various sets of images for each mission were processed applying the Python module (Agisoft, 2022) integrated into the Agisoft Metashape 2.0.1. program (Agisoft, 2023) with identical settings. For each mission, an orthomosaic and a 3D point cloud were generated. In the first step, the images captured during Block 2 of each mission were processed. In the next steps, images from each mission were systematically omitted, in a similar manner to Sadeq (2019 and Bupathy et al. (2021). Thus image sets were created that contained all the photos that would have been taken in Block 2 if the UAV had taken photos only at every 4, 6, 8 or 10 meters. For each image set, forward overlap values were calculated (Table 3).

Table 3. Forward overlap for each image set

Distance betw. photos [m]		2	4	6	8	10
		Overlap [%]				
Altitude	**7.5**	69%	40%	13%	–	–
[m]	**10.0**	77%	55%	32%	13%	–
	12.0	83%	65%	49%	31%	14%

In the investigation, numerous parameters have been assessed in order to be able to compare the quality of the resulting point clouds. Horizontal accuracy was checked by measuring the distances between the chartreuse markers on each point cloud, and comparing the values to the real-life measurements.

https://doi.org/10.55343/CogSust.20674

Also, the road surface in the point cloud was checked for gaps, i.e. regions devoid of generated points. If a gap with a diameter more than 10 cm on the road surface was identified in the point cloud, the point cloud was regarded as unsatisfactory. Conversely, if occasional gaps below this specified diameter were observed, the point cloud was deemed satisfactory (Figure 4). The limit of 10 cm was determined based on the fact that for accident scene documentation, occasional gaps of such small size are not disturbing. Notably, skid marks and other evidentiary features highlighted by the police typically exceed the aforementioned 10 cm threshold.

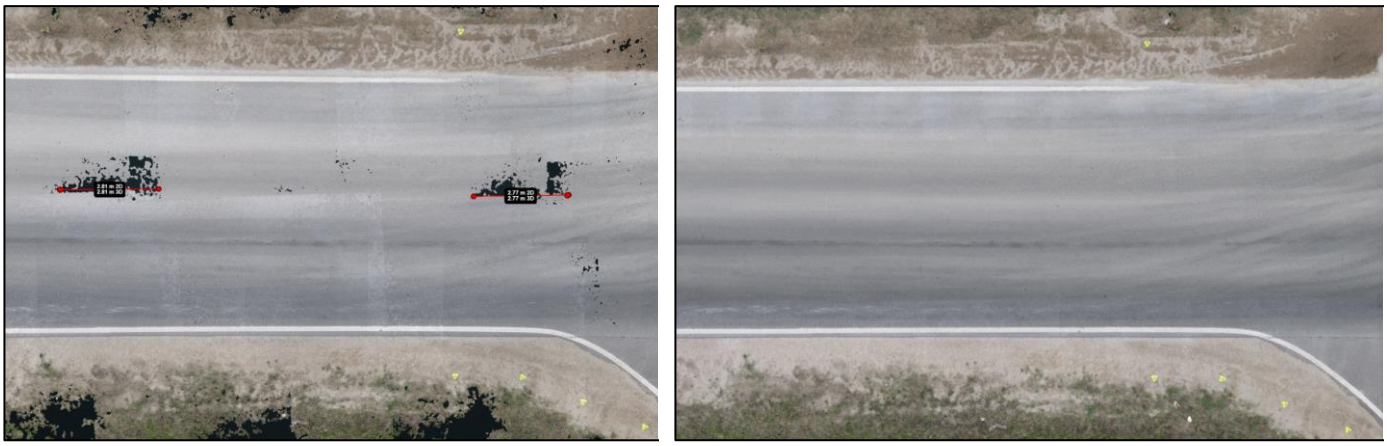

(**a**) (**b**)

Figure 4. Gap detection in a point cloud. **a)** Gaps larger than 10 cm – unsatisfactory. **b)** no gaps – satisfactory

In addition to evaluating point cloud quality, the metadata associated with each mission were analyzed. The parameters considered in this scrutiny included the number of images, the overall size of the image set, processing time, and the resultant size of the point cloud. The data were extracted from the processing report provided by the processing software for each mission.

In order to assess the viability of utilizing the 3D point clouds deemed satisfactory by the above methods for accident simulation purposes, the point clouds were exported to the Virtual Crash 5 simulation software (Virtual Crash, n.d.). Subsequently, a 3D mesh surface was generated for each point cloud, thereby establishing a simulation environment. It was checked whether the arising 3D mesh surface is geometrically correct compared to the actual site. The aim was to test whether the quality of the 3D mesh surface is satisfactory for the reconstruction of a hypothetical accident at the junction recorded. This is why the accident reconstruction software Virtual Crash was applied, although several other software programs may be used to generate such 3D mesh surfaces (such as Maya (Autodesk, n.d.b), 3DS Max (Autodesk, n.d.a), Blender (n.d.). Figure 5 summarizes the steps of the experiment.

https://doi.org/10.55343/CogSust.20674

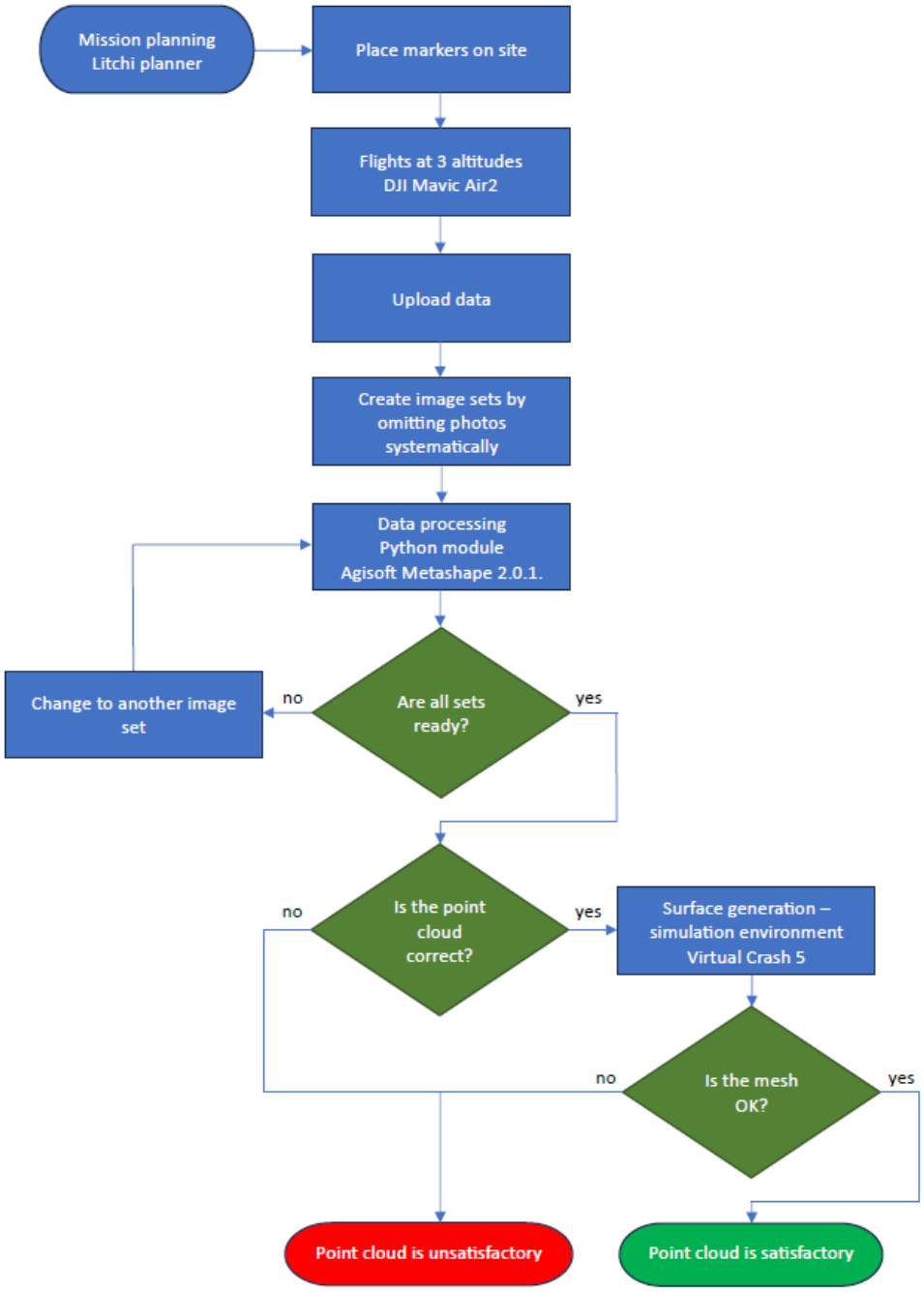

Figure 5. Experimental design.

3. Results

In this section, the results of a comprehensive analysis of the literature are followed by the results of the field tests.

3.1 Analysis of the literature

In the preliminary phase of the present research, several publications using UAV imagery with different purposes have been reviewed, looking for optimal overlap values. Table 4 shows the different forward overlap values reported for varied terrains and mission objectives.

https://doi.org/10.55343/CogSust.20674

Table 4. Overlap values reported in the literature for missions on different types of terrains.[1]

type of area	altitude [m]	forward overlap %	Source
forest	20, 40, 60, 80	60–96, every 4%	Dandois et al. 2015
pine forest	90, 120	**90**, 95	Young et al. 2022
tropical woodland	286, 487	90	Domingo et al. 2019
olive orchard	50, **100**	**95**, 97 58, 64, 69	Torres-Sánchez et al. 2017
desert	140, 160, 180, 200	60–70–**80**	Elhadary et al. 2022
rosemary scrub	60	85	Charton et al. 2021
university campus	60	80–>65 vertical 91–>76 oblique	Sadeq 2019
aubergine field	13, 15	90	Bupathy et al. 2021
wetlands	60, 80, 100, **120**	40, 50, **60**, 70, 80, 90	Flores-de-Santiago et al. 2020
snow depth	**50**, 100	70, **80**, 90	Lee et al. 2021
vertical quarry wall	horizontal: 20	80	Grohmann et al. 2023
sloping cliff face	horizontal: 40–60	70 85	Goncalves et al. 2021
bridges		66.7	Wang et al 2022
archeological site	**15**, 45, 75	60, 70, **80**	Luis-Ruiz et al 2021
road accident	20 25	80	Pádua et al. 2021
	15	–90	Mat Amin et al 2020
	15	80–90	Zulkifli and Tahar 2023

[1] Bold figures show the values that were regarded as the optimal ones in the referenced article.

Based on the values published in the above articles, Figure 6 was generated to show what forward overlap percentages were tested and what optimal overlap values were reported.

https://doi.org/10.55343/CogSust.20674

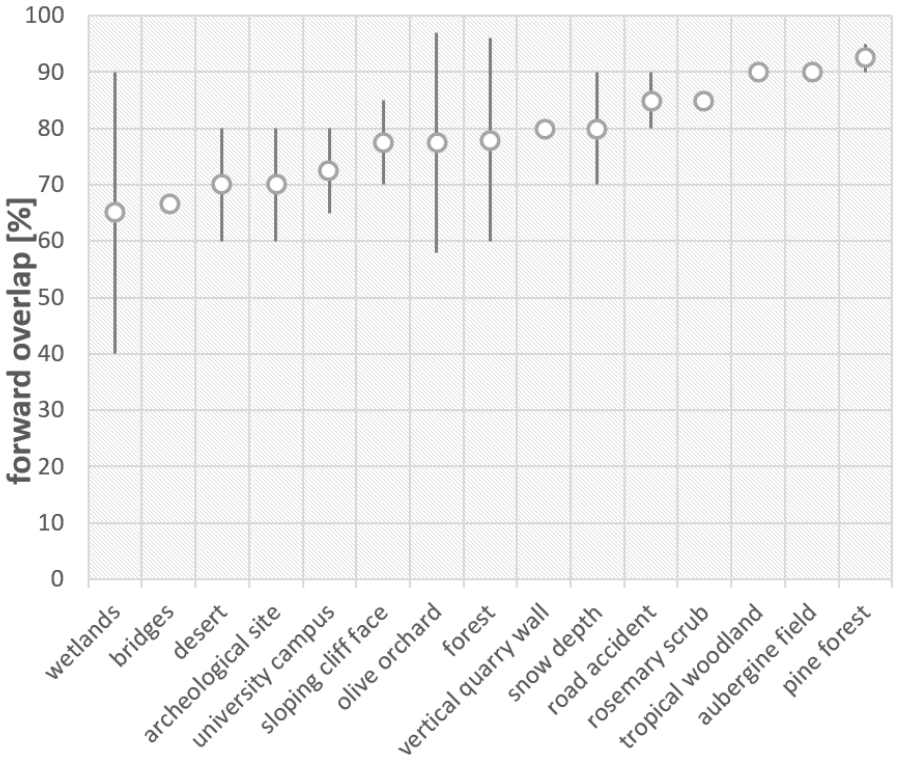

Figure 6. Forward overlap ranges in percentage according to terrain as reported in the literature, based on Table 1. Circles indicate optimal or in the lack of that, average overlap percentage

The question arises whether it is possible to identify characteristics of the terrain that dictate the optimal forward overlap for UAV missions conducted over diverse landscapes. Based on the above data and insight from relevant literature (Singh and Frazier, 2018; Seifert et al., 2019), two factors were taken into consideration. The first factor is diversity, denoting the inhomogeneity of the surface. The second factor is relief, which shows how varied elevations are on a given surface. An examination of the data in Table 4 suggests that both low diversity and substantial differences in elevation necessitate higher overlaps, as in the case of forests, where tree heights differ considerably. However, when diversity is high and elevation differences are low, as exemplified by wetlands, a reduced UAV image overlap may still yield satisfactory results (Figure 7). It is crucial to acknowledge that values in Figure 7 are approximations and serve as indicative benchmarks.

https://doi.org/10.55343/CogSust.20674

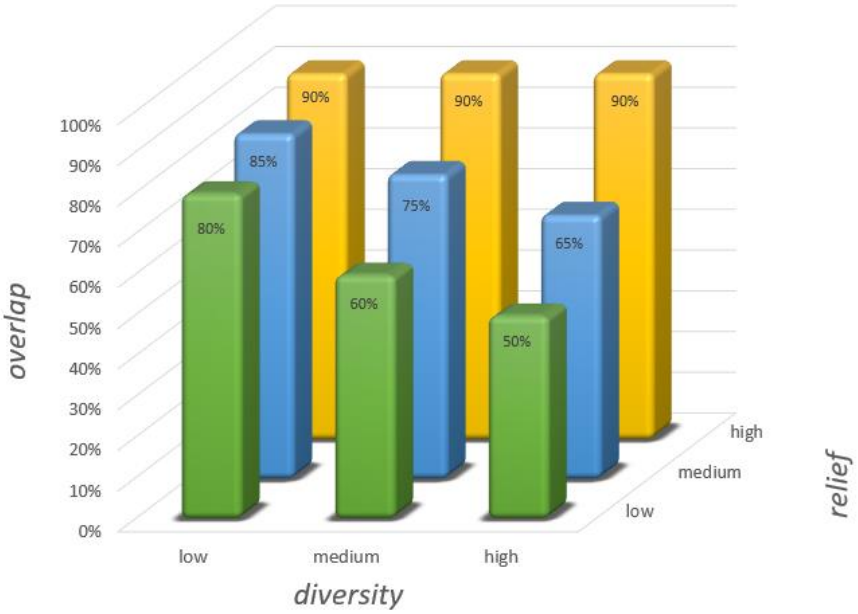

Figure 7. Forward overlap required for different terrains. The values are approximate values based on the data from Table 1

3.2 Experiment

The experiment comprised 3 missions at the altitudes of 7.5, 10 and 12 meters, with images being captured at every 2 meters. The original datasets underwent a process in which images were omitted systematically, until no forward overlap persisted between consecutive images. As a result of this procedure, a total of 12 datasets were examined: 3 sets for the 7.5 m altitude, 4 sets for the 10 m altitude, and 5 sets for the 12 m altitude (see Table 3 above). The results of the quality checks are elaborated below.

3.1. Accuracy

The accuracy of the point clouds was checked in two ways.

3.1.1. Horizontal accuracy

The horizontal accuracy of the point clouds was tested by measuring the distances on each point cloud between the chartreuse markers (Figure 8). Results are given in Table 5. The values show that the horizontal accuracy of the point clouds varies. However, from this dataset, no clear relationships can be found between overlap percentages, flight altitude and accuracy. In order to explore such relationships, further experiments must be conducted. However, as the differences between point cloud measurement results and on site measurement data are within the 0–5 cm range, the accuracy of each point cloud is satisfactory for road accident simulation purposes.

https://doi.org/10.55343/CogSust.20674

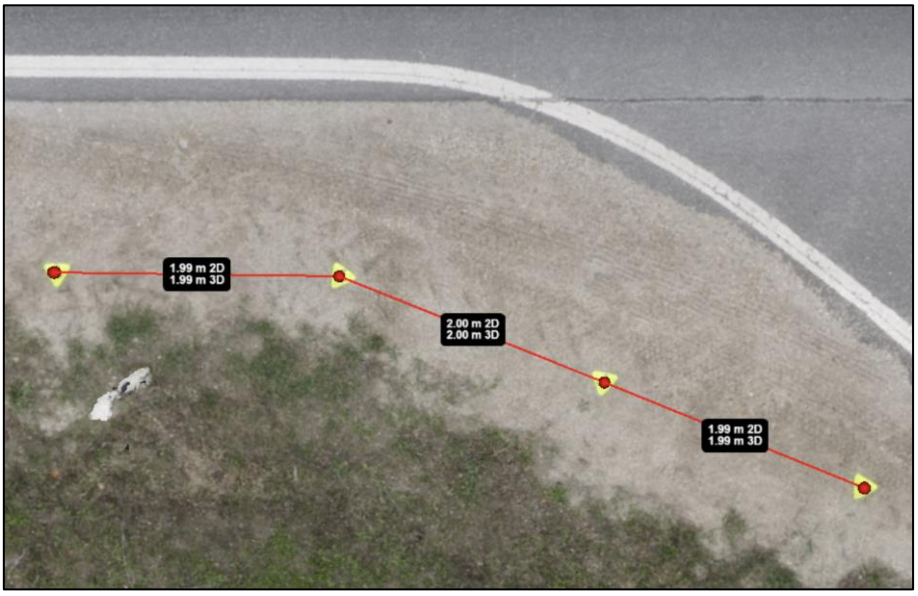

Figure 8. Measuring the distance between the chartreuse markers in the point cloud.

Table 5. Distances between the chartreuse markers measured on the point clouds. In reality, the distance between the markers was 2.00 m, measured by a laser measure.

Distance betw. photos [m]		**2**	**4**	**6**	**8**	**10**
		Measured values in point cloud [m]				
Altitude [m]	**7.5**	2.00	2.04	2.03	–	–
		2.00	2.04	2.01		
		2.01	2.04	2.01		
	10.0	2.00	1.95	2.03	2.01	–
		2.01	1.94	2.04	2.01	
		2.00	1.95	2.03	2.00	
	12.0	1.99	1.95	2.04	2.02	2.00
		2.00	1.94	2.04	2.05	2.01
		1.99	1.95	2.03	2.04	2.03

3.1.2. Gaps

Regarding gaps in the point clouds, those with gap sizes not exceeding 10 cm in diameter *(d)* were regarded as satisfactory (Table 6). In subsequent tables, those sets that were deemed satisfactory from this respect appear with a gray background colour.

Table 6. Gaps in point clouds – bold faced sets did not contain large ($d > 10$ cm) gaps.

Distance betw. photos [m]		**2**	**4**	**6**	**8**	**10**
		Overlap [%]				
Altitude [m]	**7.5**	**69%**	40%	13%	–	–
	10.0	**77%**	**55%**	32%	13%	–
	12.0	**83%**	**65%**	**49%**	31%	14%

https://doi.org/10.55343/CogSust.20674

3.2. Metadata

Each of the 12 datasets was processed with Agisoft Metashape 2.0.1 software (2023) using the same settings. Tables 7 and 8 show the sizes of the image sets and of the point clouds, respectively. This is an important metric, as storing large datasets requires large storage capacities. Additionally, the larger a data set is, the longer the processing time (Table 9).

Table 7. Number of images and size of image sets.

Distance betw. photos [m]		2	4	6	8	10
		No. of images – size of image set				
Altitude [m]	7.5	133 – 601 MB	67 – 303 MB	44 – 199 MB	–	–
	10.0	132 – 627 MB	66 – 314 MB	44 – 210 MB	33 – 156 MB	–
	12.0	93 – 487 MB	47 – 246 MB	31 – 163 MB	24 – 126 MB	19 – 100 MB

Table 8. The size of the generated point clouds.

Distance betw. photos [m]		2	4	6	8	10
		Size of the point cloud [px]				
Altitude [m]	7.5	57 814 351	37 011 874	26 898 031	–	–
	10.0	40 653 230	28 016 162	20 309 524	15 442 673	–
	12.0	24 663 121	19 154 362	15 254 324	12 851 936	10 837 981

Table 9. Processing time per image set.

Distance betw. photos [m]		2	4	6	8	10
		Processing time				
Altitude [m]	7.5	7m 39s	4m 47s	3m 39s	–	–
	10.0	6m 52s	4m 1s	2m 54s	2m 40s	–
	12.0	4m 43s	2m 41s	2m 1s	1m 40s	1m 30s

3.3. Mesh as a simulation environment

Vehicle motion simulation software generates the 3D environment from a point cloud or mesh model. In the present case, Virtual Crash 5 vehicle motion simulation software was utilized to evaluate the usability of point clouds. After importing a point cloud into the program, the program generates a 3D mesh surface from it. The arising mesh surface is then used for performing the simulation

https://doi.org/10.55343/CogSust.20674

calculations. During the mesh surface generation process, the mesh surface design can be influenced by setting a number of parameters. However, in all cases a point cloud of sufficient quality is a prerequisite for the creation of a suitable mesh model.

All the mesh surfaces generated from the point clouds that had been categorized as “satisfactory” based on their accuracy and the presence or absence of gaps (Table 6) resulted in a suitable mesh. Figure 9 shows an example for a mesh surface generated form a suitable point cloud. Vehicle movement can be accurately modeled on the mesh, including the vehicle’s descent into the ditch along the roadway.

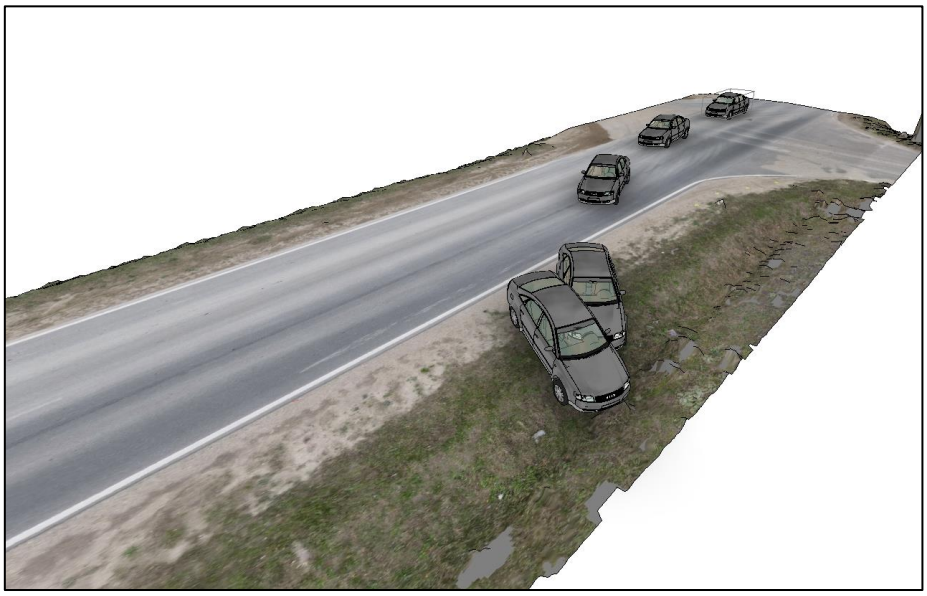

Figure 9. Mesh surface generated from the point cloud with Virtual Crash 5 software. The simulation of a roadway departure accident.

4. Discussion

The analysis of the literature confirmed Singh and Frazier (2018)’s finding that a high variability is attested in the photo overlap values used across varied UAV applications. It was proposed that the necessary overlap value may be determined by examining the vertical fragmentation (relief) and diversity of the terrain to be surveyed. Based on these characteristics of the terrain, approximate forward overlap values were suggested (Figure 9). In applications where processing time, the size of the image set and the result of the point cloud are of primary importance, the minimal overlap ratio should be used at which the quality of the resulting point cloud is still satisfactory.

Accident scene documentation is an application of UAVs where processing time and data file size should be minimized. Generally, a forward overlap ratio of 80–90% is proposed in the literature (Pádua et al., 2020; Mat Amin, 2020; Zulkifli and Tahar, 2023; Pérez, 2024) for road accident scene documentation. In contrast, our analysis has shown that for an average accident scene (straight roadway section, roadside ditch with vegetation), the point cloud resulting from processing images of at least 50% forward overlap is of sufficient quality for further processing. This also means that the number of images taken during the survey and the storage space required for archiving can be reduced by about a third. The time required to process the images can be reduced by about 50%, and the size of the resulting point cloud by about 40%. Our tests have also shown that a point cloud with about 50% overlap provides a good input for a vehicle motion simulation program to generate the 3D environment for vehicle motion calculations.

https://doi.org/10.55343/CogSust.20674

5. Conclusion

This study examined the optimal forward overlap ratio for images captured by drones during the documentation of road accident sites. Tests conducted at a road junction in Hungary suggest that a 50% forward overlap between images yields a sufficient point cloud. This relatively low overlap helps minimize the number of images captured, thereby accelerating the documentation process. A faster yet still effective accident documentation procedure shortens road closure time, resulting in reduced congestion and a more sustainable data collection process.

Author contributions: Conceptualization, GV, GM, NW; methodology, GV, GM, NW; software, GV; validation, GM, ÁT; formal analysis, GV,GM; investigation, GV, NW; resources, GV, NW; data curation, GV; writing—original draft preparation, NW; writing—review and editing, GV, ÁT; visualization, GV; supervision, GM, ÁT; project administration, GV; funding acquisition, GV. All authors have read and agreed to the published version of the manuscript.

Funding: This research was funded by NKFIH, grant number 2021-1.1.4-GYORSÍTÓSÁV-2022-00023 "Proper documentation and evaluation of an accident scene using high-performance image capture technology. Development and market introduction of an intelligent Geographic Information System (GIS) [Baleseti helyszín megfelelő dokumentálása és kiértékelése nagyteljesítményű képi adatrögzítő technológia alkalmazásával. Intelligens Térinformatikai Rendszer (ITR) kifejlesztése, piaci bevezetése]."

Conflicts of Interest: The authors declare no conflict of interest. The funders had no role in the design of the study; in the collection, analyses, or interpretation of data; in the writing of the manuscript; or in the decision to publish the results.

References

Agisoft. (2022). *Metashape Python Reference*. Release 2.0.0. URL: https://www.agisoft.com/pdf/metashape_python_api_2_0_0.pdf

Agisoft. (2023). *Agisoft Metashape 2.0.1*. URL: https://www.agisoft.com/features/professional-edition/

Autodesk. (n.d.a). *3DS Max*. URL: https://www.autodesk.com/products/3ds-max/overview?term=1-YEAR&tab=subscription

Autodesk. (n.d.b). *Autodesk Maya software*. URL: https://www.autodesk.com/products/maya/overview?term=1-YEAR&tab=subscription

Bisio, I., Garibotto, C., Haleem, H., Lavagetto, F., Sciarrone, A. (2022). A Systematic Review of Drone Based Road Traffic Monitoring System. *IEEE Access*. 10, 101537-101555. DOI: https://doi.org/10.1109/ACCESS.2022.3207282

Bupathy, P., Sivanpillai, R., Sajithvariyar, V., Sowmya, V. (2021). Optimizing low-cost UAV aerial image mosaicing for crop growth monitoring. *The International Archives of the Photogrammetry, Remote Sensing and Spatial Information Sciences*. XLIV-M-3-2021. URL: https://isprs-archives.copernicus.org/articles/XLIV-M-3-2021/7/2021/isprs-archives-XLIV-M-3-2021-7-2021.pdf

Castro, J., Morales-Rueda, F., Alcaraz-Segura, D., Tabik, S. (2023). Forest restoration is more than firing seeds from a drone. *Restoration Ecology*. 31(1), e13736. DOI: https://doi.org/10.1111/rec.13736

Charton, K., Sclater, V., Menges, E. (2021). Mapping spatially explicit vegetation gaps in Florida rosemary scrub using unmanned aerial vehicles. *Ecosphere*. 12(4). DOI: https://doi.org/10.1002/ecs2.3470

Virtual Crash (n.d.). *Virtual Crash 5 Accident Reconstruction Software*. URL: https://www.vcrashusa.com/vc5

Dandois, J., Olano, M., Ellis, E. (2015). Optimal altitude, overlap, and weather conditions for computer vision UAV estimates of forest structure. *Remote Sensing*. 7(10), 13895-13920. DOI: https://doi.org/10.3390/rs71013895

Desai, J., Mathew, J. K., Zhang, Y., Hainje, R., Horton, D., Hasheminasab, S. M., Habib, A., Bullock, D. M. (2022). Assessment of Indiana Unmanned Aerial System Crash Scene Mapping Program. *Drones*. 6(259), 1-15. DOI: https://doi.org/10.3390/drones6090259

DJI. (n.d.). *Mavic Air 2*. URL: https://www.dji.com/hu/mavic-air-2/specs

Domingo, D., Ørka, H., Næsset, E., Kachamba, D., Gobakken, T. (2019). Effects of UAV Image Resolution, Camera Type, and Image Overlap on Accuracy of Biomass Predictions in a Tropical Woodland. *Remote Sensing*. 11(8), 948. DOI: https://doi.org/10.3390/rs11080948

https://doi.org/10.55343/CogSust.20674

El Hummaidi, L. L. (2021). Using unmanned aerial systems and deep learning for agriculture mapping. *Heliyon*. 7, e08154. DOI: https://doi.org/10.1016/j.heliyon.2021.e08154

Elhadary, A., Rabah, M., Ghanim, E., Mohie, R., Taha, A. (2022). The influence of flight height and overlap on UAV imagery over featureless surfaces and constructing formulas predicting the geometrical accuracy. *NRIAG Journal of Astronomy and Geophysics*. 11(1), 210–223. DOI: https://doi.org/10.1080/20909977.2022.2057148

Flores-de-Santiago, F., Valderrama-Landeros, L., Rodríguez-Sobreyra, R. (2020). Assessing the effect of flight altitude and overlap on orthoimage generation for UAV estimates of coastal wetlands. *Journal of Coastal Conservation*. 24, 35. DOI: https://doi.org/10.1007/s11852-020-00753-9

Blender (n.d.). *Blender*. URL: https://www.blender.org/download/

Gonçalves, G., Gonçalves, D., Gómez-Gutiérrez, Á., Andriolo, U., Pérez-Alvárez, J. (2021). 3D reconstruction of coastal cliffs from fixed-wing and multi-rotor uas: impact of SfM-MVS processing parameters, image redundancy and acquisition geometry. *Remote Sensing*. 13(6), 1222. DOI: https://doi.org/10.3390/rs13061222

Grohmann, C. H., Viana, C. D., Garcia, G. P., Albuquerque, R. W. (2023). Remotely piloted aircraft-based automated vertical surface survey. *MethodsX*. 10. DOI: https://doi.org/10.1016/j.mex.2022.101982

James, M. R., Antoniazza, G., Robson, S., Lane, S. N. (2020). Mitigating systematic error in topographic models for geomorphic change detection: accuracy, precision and considerations beyond off-nadir imagery. *Earth Surface Processes and Landforms*. 45, 2251–2271. DOI: https://doi.org/10.1002/esp.4878

Lee, S., Park, J., Choi, E., Kim, D. (2021). Factors Influencing the Accuracy of Shallow Snow Depth Measured Using UAV-Based Photogrammetry. *Remote Sensing*. 13(4), 828. DOI: https://doi.org/10.3390/rs13040828

Litchi. (2023). *Litchi for DJI Drones*. URL: https://flylitchi.com/

Liu, X., Lian, X., Yang, W., Wang, F., Han, Y., Zhang, Y. (2022). Accuracy Assessment of a UAV Direct Georeferencing Method and Impact of the Configuration of Ground Control Points. *Drones*. 6(2), 30. DOI: https://doi.org/10.3390/drones6020030

Luis-Ruiz, J., Sedano-Cibrián, J., Pereda-García, R., Pérez-Álvarez, R., Malagón-Picón, B. (2021). Optimization of Photogrammetric Flights with UAVs for the Metric Virtualization of Archaeological Sites. Application to Juliobriga (Cantabria, Spain). *Applied Sciences*. 11(3), 1204. DOI: https://doi.org/10.3390/app11031204

Mat Amin, A., Abdullah, A., Abdul Mukti, S., Moht Zaidi, M., Tahar, K. (2020). Reconstruction of 3D accident scene from multirotor UAV platform. *The International Archives of the Photogrammetry Remote Sensing and Spatial Information Sciences*. XLIII-B2-2020, pp. 451–458. DOI: https://doi.org/10.5194/isprs-archives-XLIII-B2-2020-451-2020

Michail, A. L. (2024). A comprehensive review of unmanned aerial vehicle-based approaches to support photovoltaic plant diagnosis. *Heliyon*. 10, e23983. DOI: https://doi.org/10.1016/j.heliyon.2024.e23983

Nomikos, N., Gkonis, P. K, Bithas, P. S., Trakadas, P. (2023). A Survey on UAV-aided maritime communications: Deployment considerations, applications, and future challenges. *IEEE Open Journal of the Communications Society*. 4, 56–78. DOI: https://doi.org/10.1109/OJCOMS.2022.3225590

Nesbit, P. R., Hugenholtz, C. H. (2019). Enhancing UAV–SfM 3D model accuracy in high-relief landscapes by incorporating oblique images. *Remote Sensing*. 11(3), 239. DOI: https://doi.org/10.3390/rs11030239

Pádua, L., Sousa, J., Vanko, J., Hruška, J., Adão, T., Peres, E., Soua, A., Sousa, J. J. (2020). Digital reconstitution of road traffic accidents: A flexible methodology relying on UAV surveying and complementary strategies to support multiple scenarios. *International Journal of Environmental Research and Public Health*. 17(6). DOI: https://doi.org/10.3390/ijerph17061868

Pérez, J. A., Gonçalves, G. R., Morillo Barragán, J. R., Fuentes Ortega, P., Caracol Palomo, A. A. (2024). Low-cost tools for virtual reconstruction of traffic. *Heliyon*. 10, e29709. DOI: https://doi.org/10.1016/j.heliyon.2024.e29709

Sadeq, H. A. (2019). Accuracy assessment using different UAV image overlaps. *Journal of Unmanned Vehicle Systems*. 7(3), 175–193. DOI: https://doi.org/10.1139/juvs-2018-0014

Sanz-Ablanedo, E., Chandler, J. H., Ballestros-Pérez, P., Rodriguez-Pérez, J. R. (2020). Reducing systematic dome errors in digital elevation models through better UAV flight design. *Earth Surface Processes and Landforms*. 45(9), 2143-2147. DOI: https://doi.org/10.1002/ESP.4871

https://doi.org/10.55343/CogSust.20674

Seifert, E., Seifert, S., Vogt, H., Drew, D., van Aardt, J., Kunneke, A., Seifert, T. (2019). Influence of drone altitude, image overlap, and optical sensor resolution on multi-view reconstruction of forest images. *Remote Sensing*. 11(10), 1252. DOI: https://doi.org/10.3390/rs11101252

Singh, K. K., Frazier, A. E. (2018). A meta-analysis and review of unmanned aircraft system (UAS) imagery for terrestrial applications. *International Journal of Remote Sensing*. 39(15–16), 5078-5098. DOI: https://doi.org/10.1080/01431161.2017.1420941

Stott, E., Williams, R. D., Hoey, T. B. (2020). Ground control point distribution for accurate kilometre-scale topographic mapping using an RTK-GNSS unmanned aerial vehicle and SfM photogrammetry. *Drones*. 4(3), 55. DOI: https://doi.org/10.3390/drones4030055

Torres-Sánchez, J., López-Granados, F., Bprra-Serrano, I., Peña. (2018). Assessing UAV-collected image overlap influence. *Precision Agriculture*. 19, 115–133. DOI: https://doi.org/10.1007/s11119-017-9502-0

Török, Á., Bögöly, G., Somogyi, Á., Lovas, T. (2020). Application of UAV in topographic modelling and structural geological mapping of quarries and their surroundings – delineation of fault-bordered raw material reserves. *Sensors*. 20. DOI: https://doi.org/10.3390/s20020489

Wang, F., Zou, Y., Del Rey Castillo, E., Lim, J. P. (2022). Optimal UAV image overlap for photogrammetric 3D reconstruction of bridges. *IOP Conference Series: Earth and Environmental Science.* 1101, 022052. DOI: https://doi.org/10.1088/1755-1315/1101/2/022052

Young, D. J., Koontz, M., Weeks, J. (2022). Optimizing aerial imagery collection and processing parameters for drone-based individual tree mapping in structurally complex conifer forests. *Methods in Ecology and Evolution*. 13(7), 1447–1463. DOI: https://doi.org/10.1111/2041-210X.13860

Zulkifli, M. H., Tahar, K. N. (2023). The Influence of UAV Altitudes and Flight Techniques in 3D Reconstruction Mapping. *Drones*. 7(4), 227. DOI: https://doi.org/10.3390/drones7040227